

Mocap-2-to-3: Lifting 2D Diffusion-Based Pretrained Models for 3D Motion Capture

Zhumei Wang¹ Zechen Hu^{1*} Ruoxi Guo² Huaijin Pi^{2,3} Ziyong Feng¹ Sida Peng²
Xiaowei Zhou²

¹Deep Glint ²Zhejiang University ³The University of Hong Kong

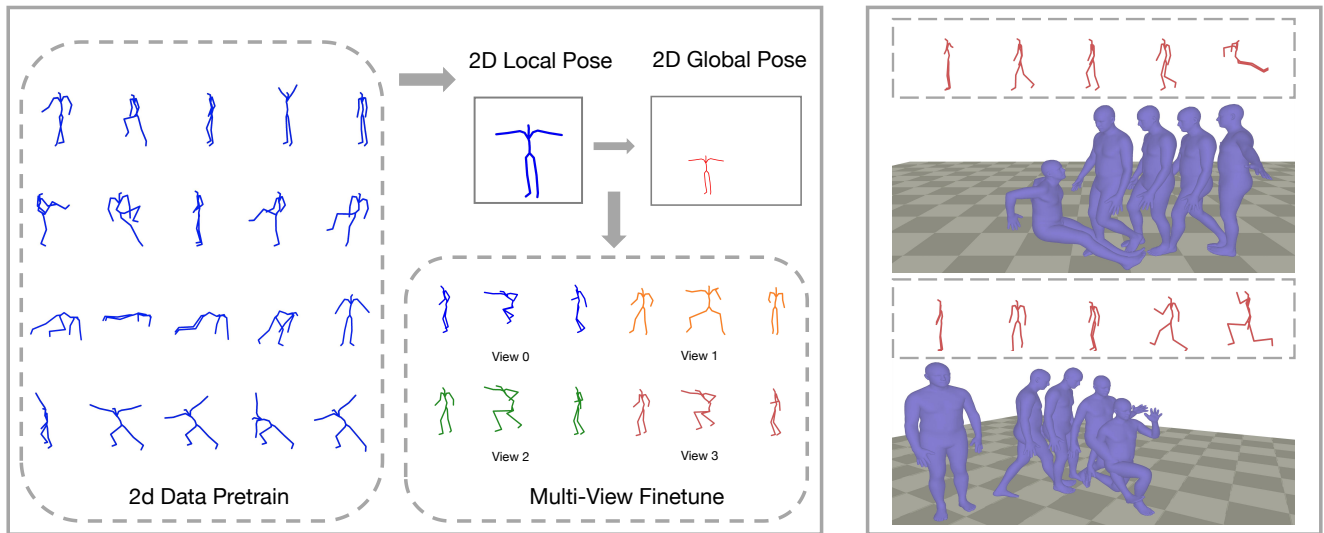


Figure 1. **Illustration of our key idea.** Left side: training process; right side: inference process. Mocap-2-to-3 can generate 3D motions with absolute positions in the world coordinate system based on monocular 2D cues. The training process consists of two phases: a 2D pretraining phase and a multi-view finetune phase. During the 2D phase, arbitrary self-collected data can be incorporated to improve the effectiveness of the 3D motion results.

Abstract

Recovering absolute poses in the world coordinate system from monocular views presents significant challenges. Two primary issues arise in this context. Firstly, existing methods rely on 3D motion data for training, which requires collection in limited environments. Acquiring such 3D labels for new actions in a timely manner is impractical, severely restricting the model’s generalization capabilities. In contrast, 2D poses are far more accessible and easier to obtain. Secondly, estimating a person’s absolute position in metric space from a single viewpoint is inherently more complex. To address these challenges, we introduce Mocap-2-to-3, a novel framework that decomposes intricate 3D motions into

2D poses, leveraging 2D data to enhance 3D motion reconstruction in diverse scenarios and accurately predict absolute positions in the world coordinate system. We initially pretrain a single-view diffusion model with extensive 2D data, followed by fine-tuning a multi-view diffusion model for view consistency using publicly available 3D data. This strategy facilitates the effective use of large-scale 2D data. Additionally, we propose an innovative human motion representation that decouples local actions from global movements and encodes geometric priors of the ground, ensuring the generative model learns accurate motion priors from 2D data. During inference, this allows for the gradual recovery of global movements, resulting in more plausible positioning. We evaluate our model’s performance on real-world datasets, demonstrating superior accuracy in motion

*Corresponding author.

and absolute human positioning compared to state-of-the-art methods, along with enhanced generalization and scalability. Our code will be made publicly available.

1. Introduction

Our goal is to recover human motion and absolute positions in world coordinates from monocular images with a fixed camera. This markerless motion capture has broad applications in gaming, sports analysis, multi-person interactions, and embodied intelligence. Compared to multi-view reconstruction, monocular methods have lower hardware requirements and fewer environmental constraints, making them more suitable for downstream tasks [27]. Current state-of-the-art methods [25, 26, 29–31, 39] heavily rely on precise 3D motion capture data [1, 8, 21, 22], which is costly and challenging to acquire. This process requires specialized marker devices and controlled environments, making it inaccessible for many research institutions. Most critically, in practice, 3D data acquisition is constrained by complex processes, affecting timeliness, and swiftly collecting out-of-distribution 3D data to promptly address downstream application issues is nearly unfeasible. In contrast, 2D data is more accessible, as it can be sourced from internet videos, offering diverse motion styles and real-world actions [23], or captured in specific scenarios with 2D skeletons provided through manual annotation or pose estimators [37, 39].

Moreover, although previous methods have addressed certain issues, they fail to comprehend the 3D spatial relationships within the world. Most existing approaches can only predict relative positions within the camera coordinate system, where they evaluate by aligning the root and scaling the human body, or by performing first-frame alignment. Predicting the absolute 3D positions in the world coordinate system is more challenging [38]. Effective absolute positioning has broader applications, as it necessitates an awareness of the 3D environment and the reasoning of positional relationships to infer complex behavioral interactions. For instance, determining whether two individuals are engaged in a fight in a public space relies on the absolute positions in the world coordinate system to ascertain the state of interaction.

Based on this, we propose a novel framework, Mocap-2-to-3, which constructs a robust 3D strategy by enhancing 2D pretrained data and 3D spatial perception capabilities. We decompose complex 3D motions into 2D poses and introduce a 2D-lifting strategy, enabling the architecture to leverage 2D data to improve the generalization ability of the motion model in new scenarios. Recent work [16] suggested using only 2D pose sequences for training, employing a multi-stage framework to gradually recover accurate global 3D motion. However, relying solely on 2D data is not the approach we advocate. We believe that 3D

data inherently possesses advantages: accurate absolute positioning, motion coordination, and consistency in skeletal proportions. As evidenced by the experimental conclusions of [16], models trained exclusively with 2D data cannot surpass those trained with 3D data in terms of motion quality. Therefore, we do not intend to discard 3D data; instead, we aim to augment the limited 3D data with 2D data to enhance generalization for new tasks. This approach ensures that our model achieves optimal performance in both accuracy and generalization.

As illustrated in Fig. 1, inspired by [23], we adopt a pre-training approach that utilizes existing 2D data to train a single-view diffusion model. To recover 3D human motion, we fine-tune a multi-view diffusion model using 3D data. During the inference phase, the multi-view diffusion model progressively recovers view-consistent 3D motion through triangulation. Specifically, given the 2D pose from the observed view and the camera’s parameters, the diffusion model generates 2D poses from other viewpoints, which are then lifted to 3D motion.

Nevertheless, directly generating global motion for each viewpoint is not the optimal solution. Due to the fact that positional errors between poses are significantly larger than joint errors, the model struggles to learn subtle motion variations effectively, leading to sliding artifacts across different viewpoints. To address this issue, we propose a novel human motion representation that disentangles local actions from global movements. The network learns normalized local 2D poses within bounding boxes while simultaneously learning a set of additional global variables. During inference, the local poses are mapped to global poses to restore the overall motion. Furthermore, we explicitly model the mapping relationship between 2D human positions and the ground, minimizing the loss of spatial information and thereby generating more plausible locations.

Our architecture is designed based on real-world application scenarios. For any new scenario that requires scalability, it only necessitates camera calibration, followed by the incorporation of camera parameters into the training process. When training data lacks certain actions, adding monocular 2D data during pre-training enhances 3D motion effectiveness. This lifting approach shows better generalization than traditional 3D methods, even without same-distribution data. Our model lifts any 2D pose format (e.g., SMPL [7], COCO [19], H36M [8], etc.) to 3D, requiring only retargeting the training set to the desired format. This paper focuses on improving the 2D to 3D lifting process. In our evaluations, additional errors resulting from significant deviations from the truth in general 2D detectors are beyond the scope of this work, as we do not input images and therefore do not perform secondary corrections. By not linking images to 3D motion, we leverage limited 3D data to create extensive virtual training data, boosting generalization.

In summary, our contributions are as follows: 1) We propose a pre-training approach that performs single-view pre-training on 2D data and fine-tunes for view-consistent multi-view generation on a limited 3D dataset, thereby lifting 2D pre-training to robust 3D motion. 2) We introduce a novel human motion representation that decouples local actions from global movements, enhancing 3D spatial awareness to accurately recover 3D motions and their positions in the world. 3) We validate on in-the-wild datasets that our model outperforms previous methods in both motion estimation accuracy and global positioning. Even without adding any new scene-specific data, our model demonstrates superior generalization capabilities compared to traditional methods.

2. Related work

2.1. Monocular human motion recovery

Monocular Human Motion Recovery, crucial for virtual reality, augmented reality, and human-computer interaction. HMR[10] pioneered this field by introducing an end-to-end framework that regresses SMPL [20] parameters from a single image. Subsequent works like SPIN [14] improved accuracy by integrating optimization-based refinement during training, while VIBE [12] extended this to video sequences, incorporating temporal information for smoother motion recovery. Recent methods like PAREE [13] introduced part-based attention to handle occlusions and extreme poses, and CLIFF [18] improved full-body pose estimation by incorporating global location information. In multi-person scenarios, ROMP [30] introduced a single-stage, monocular approach for efficient 3D reconstruction of multiple individuals. Current methods, such as MotionBERT [39], typically predict camera-relative offsets from the root node. Sequence-based methods like GV-HMR [25] predict global trajectories by aligning motion with gravity but often require initial frame alignment and lack absolute positions in world coordinates, highlighting ongoing challenges in global motion recovery.

2.2. Monocular 3D absolute pose estimation

Some methods achieve absolute position estimation in monocular scenarios by introducing additional environmental information. Ray3D [38] is a ray-based monocular 3D human pose estimation method that maps 2D keypoints into 3D ray space for absolute 3D localization, leveraging geometric constraints to enhance accuracy and robustness in monocular scenarios. SA-HMR [24] recovers the absolute position of human meshes by utilizing a pre-scanned scene from a single image. The joint learning of image and geometric scene information helps reduce ambiguities caused by depth and occlusion. MVLift [16] uses epipolar constraints to predict joint rotations and root trajectories, train-

ing only on 2D poses to achieve metrics close to 3D methods. In contrast, We enhance 3D mocap with 2D data, outperforming pure 3D approaches in both metrics and generalization.

2.3. Motion Generation

Some studies have explored motion generation based on diffusion models. MDM [32] introduces a diffusion-based framework for realistic human motion generation, leveraging denoising to capture complex dynamics and variability. MAS [11] utilizes 2D diffusion models in a multi-view setup for high-fidelity 3D motion generation with enhanced spatial consistency. Motion-2-to-3 [23] proposed to incorporate massive internet videos in the pre-training process to improve motion generation. We draw inspiration from this pre-training strategy to enhance motion capture tasks and introduce multi-view geometric constraints for recovering absolute poses.

3. Method

We introduce Mocap-2-to-3, a novel markerless motion capture framework designed to reconstruct global 3D motion sequences from single-view 2D poses, lifting the corresponding camera poses, as depicted in Fig. 2. Our approach begins with the pre-training of a single-view diffusion model utilizing 2D pose data. Building upon this foundation, we refine a multi-view consistent 2D diffusion model through fine-tuning with accessible 3D datasets. To ensure the precision of both motion dynamics and global positioning, our methodology distinctly separates the learning processes for motion and position. This is further enhanced by integrating pointmaps as an additional input, fostering multi-view positional consistency. Concluding our methodological exposition, we detail the inference mechanism that facilitates the transition from multi-view 2D poses to coherent 3D motion sequences.

3.1. Motion representation

Given a single view and the intrinsic and extrinsic parameters of all cameras, recovering the global 3D motion using multi-view data requires knowledge of the coordinate positions of other views in the image. However, since the influence of position on the loss is significantly greater than that of the skeleton, directly predicting the global pose tends to bias the network towards learning positional information rather than motion. This results in estimated 3D motions that do not align well with the input 2D sequences in terms of action. To address this issue, we propose a novel representation of human motion that separates local motion from global movement. Local motion refers to the 2D pose sequences within bounding boxes, denoted as local pose, while global information encompasses the center and scale

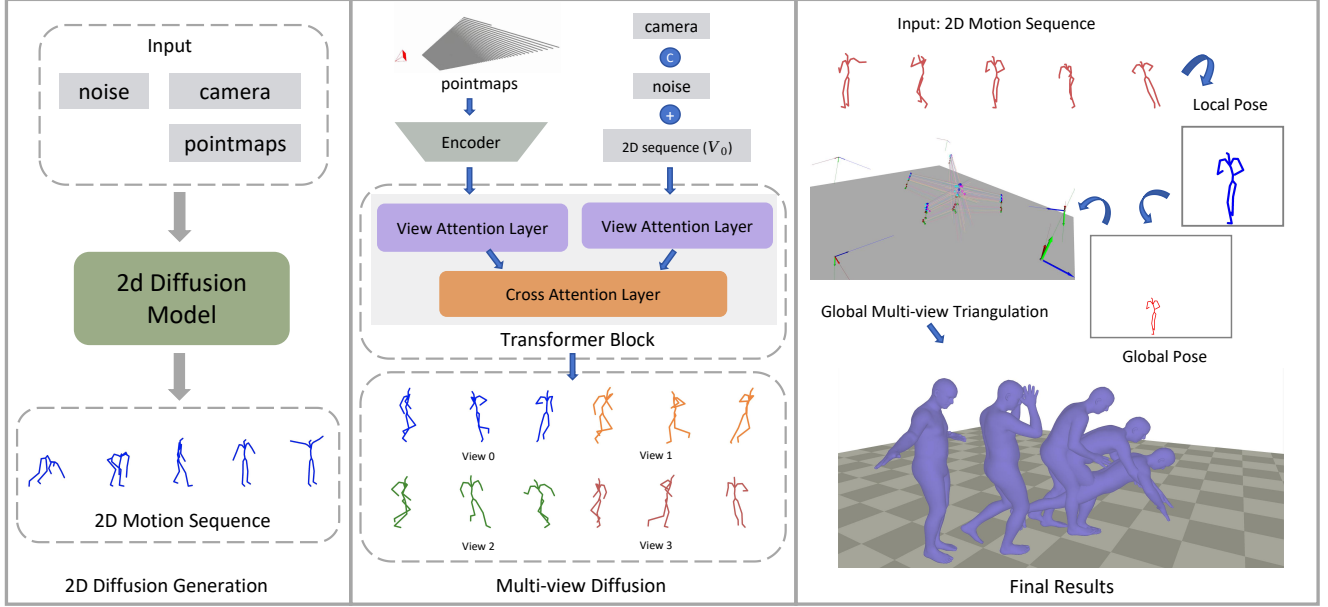


Figure 2. **Overview of the proposed framework.** The Mocap-2-to-3 diffusion model is trained in two stages. First, it predicts single-view 2D local poses and establishes monocular 3D spatial relationships using camera and ground inputs. Second, the 2D pose sequence from view 0 is added as a condition, and an Attention Layer learns multi-view geometric consistency while encoding ground-motion constraints. During inference, local poses, offsets, and scales for other views are generated based on view-0 cues. Global pose recovery and triangulation produce 3D motion with absolute positions in the world coordinate system at step T.

of the bounding boxes. The local pose is then used to reconstruct the global pose through the global information.

Given a sequence comprising T frames, we extract J points from the 2D pose, with the 2D motion represented as $M \in R^{T \times J \times 2}$, where for any j -th key point, it is denoted as (x_t^j, y_t^j) . We crop the 2D pose using bounding boxes and normalize it to the range $[-1, 1]$, positioning the root at the center of the bounding boxes, allowing the network to learn the normalized human 2D motion $M_l \in R^{T \times J \times 2}$. Additionally, we decompose the positional information into *offset* (x_t^g, y_t^g) and *scale* (w_t^g, h_t^g) . The offset represents the position of the root node in the image, and the scale corresponds to the size of the bounding boxes relative to the normalized image. Subsequently, we append this positional information to the output $M \in R^{T \times (J+2) \times 2}$. During the inference phase, the 2D motion is reconstructed into global motion using the offset and scale, resulting in more plausible positioning.

3.2. 2D motion pretrain

Existing methods for 3D motion estimation typically require 3D data as labels for training. We explore how to better generalize the model to out-of-distribution scenarios. To this end, we decompose complex 3D motion into multi-view 2D motion and divide the training into two stages: 2D and multi-view. In the first stage, the model is trained to predict 2D motion from any camera perspective. This stage

can incorporate any 2D data, such as videos collected from real-world scenarios or publicly available videos on the internet, aiming to provide a richer prior of motions from a single camera view. After training the single-view 2D diffusion model, the multi-view stage focuses solely on learning the consistency across different views, including both motion consistency and global position consistency.

This design aligns more closely with real-world application scenarios. For instance, when conducting behavioral analysis at deployment sites of a certain project, where multiple sites have similar field sizes and each site is equipped with only a single camera, we can collect 2D data from various project sites. During the pretrain phase, we focus solely on training the mapping between the single-camera pose and the camera parameters. In the second stage, cameras from multiple similar sites can be arbitrarily combined to form a virtual multi-view environment. At this stage, we only need to perform random positional augmentation on the publicly available 3D motion data, enabling the network to learn the mapping between the absolute position of the human body and the multi-view camera setup. This approach allows us to obtain more accurate 3D motion without the need for a multi-camera data acquisition system. By ensuring multi-view geometric consistency and human skeleton proportionality, we delegate the learning of motion priors to the first stage, thereby enhancing the generalization capability of our 3D motion model using only 2D data.

To train the 2D diffusion model, we incorporate two types of training data: 1) Humanml3d [4], where 2D joints are obtained by re-projecting using camera parameters, and each batch is trained on any single view; 2) 2D data that shares the same origin as the test set. Following [23, 32], we employ a transformer-based [33] diffusion model [6]. During the first stage, the network takes random noise and camera parameters as conditions and outputs a sequence of 2D motion. Since the pre-trained model learns to generate from a single view, it can leverage a large amount of 2D data as prior knowledge, enabling the network to learn motion patterns from arbitrary viewpoints. This facilitates rapid convergence in the subsequent fine-tuning phase.

3.3. Multi-view finetune

With the motion prior established, we proceed to fine-tune the 2D diffusion model in the second stage to learn consistency across multiple views. To train the multi-view diffusion model, we back-project 3D motion onto each camera view to obtain geometrically consistent 2D motion ground truth. Since additional image pairs are not required as input, we can leverage existing 3D motion and camera parameters to randomly synthesize diverse training data, thereby enhancing the model’s generalization capability in real-world scenarios.

We first determine the camera poses. Given a primary view V_0 , the other three views V_{1-3} are taken from different camera perspectives in the test set. In practical applications, any view from the 2D pretrain phase can be used to form a virtual multi-view system. We redefine the world coordinate system as shown in Fig. 3(b), where the origin of the xz -axis is directly below the focal point of the main camera V_0 , the y -axis origin is on the ground, and the xz -axis is parallel to the ground. The other cameras are represented by their rotations relative to V_0 . Within the camera bounding box, we apply random translations and rotations to the 3D motion to enhance the diversity of the training data.

Building upon the 2D diffusion model, we incorporate multi-view self-attention layers to capture consistency information across multiple views. In addition to noise as input, the 2D motion $M_0 \in R^{T \times (J+2) \times 2}$ from the V_0 view is also added to the noise, enabling the network to recover the motion and position of other views based on this guidance. Furthermore, the camera’s intrinsic parameters $K \in R^{V \times 4}$ and extrinsic parameters $Rt \in R^{V \times 3}$ are concatenated as conditions into the diffusion process, representing the camera pose, which includes the pitch angle α , roll angle β , and camera height t_y . To more accurately express the relationships between cameras, we encode the ground plane equation as pointmaps and input them into the network.

3.3.1. Multi-view pointmaps condition

The issue of depth ambiguity in monocular vision is a perennial topic of discussion. Given a viewpoint V_0 , learn-

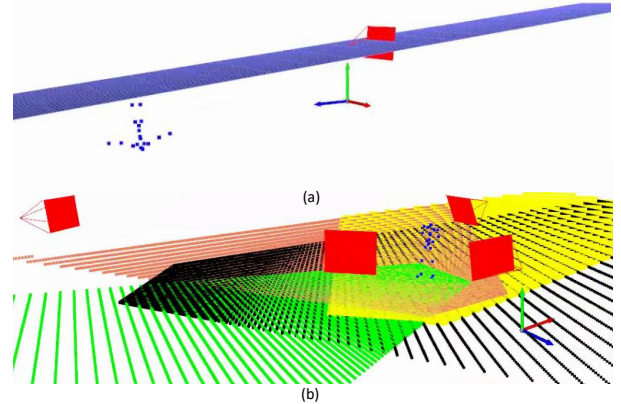


Figure 3. (a) Ground plane equation in the camera coordinate system. (b) Establishment of the world coordinate system and visualization of the pointmaps corresponding to each camera.

ing the 2D motion location from other views remains an ambiguous problem. A key idea is to incorporate the ground plane equation into the network, which helps to disambiguate the locations from other viewpoints. The ground plane equation is represented using pointmaps.

Pointmaps, introduced by [15, 35], are defined in this paper as $P \in R^{W \times H \times 3}$. They represent the (w_x, w_y, w_z) values in the world coordinate system corresponding to each pixel (u, v) on the image from any given viewpoint V , where W and H denote the width and height of the image, respectively. As mentioned earlier, the ground plane in the world coordinate system is defined as $y = 0$. This plane can be transformed into the ground plane within any camera viewpoint using the camera’s extrinsic parameters, as illustrated in Fig. 3(a), and is expressed as

$$a \times x + b \times y + c \times z + d = 0. \quad (1)$$

Where, a, b, c, d represent the coefficients of the plane. For any pixel (u, v) in the image, it can be transformed into a point (c_x, c_y) in the coordinate system using the camera’s intrinsic parameters. Following [9], given (c_x, c_y) and a, b, c, d , the depth c_z projected onto the plane can be computed. The (c_x, c_y, c_z) can then be transformed into the world coordinate system (w_x, w_y, w_z) using the camera’s extrinsic parameters. These points represent the intersections of the rays emitted from the camera’s epipole with the ground plane, and P denotes the point cloud corresponding to the ground plane for the given viewpoint. As illustrated in Fig. 3(b).

Since the ground positions in the world coordinate system corresponding to the imaging pixels of each viewpoint can be calculated solely based on the known camera parameters, a natural connection is established between the viewpoints. Unlike other methods that require environmental point cloud information as input, our approach only needs

the point cloud of the ground plane, which does not require additional equipment or computational resources to obtain, only camera calibration is necessary. Similar to images, the pointmaps are first encoded using an encoder. Then, multi-view self-attention layers are added to the diffusion model to learn the correlations between multi-view pointmaps. Finally, cross-attention is performed between M and P to guide the generation of motion.

Under the aforementioned framework, the multi-view diffusion model takes noise and conditions as inputs and outputs clean 2D motions and offsets with geometric consistency, thereby recovering realistic global motion.

3.4. Inference

For each time step t , the diffusion model takes Rt , K , M_0 , and P as inputs and outputs the predicted 2D motion $M_v \in R^{V \times T \times (J+2) \times 2}$, as described by

$$\begin{aligned} M_{vg} = M_{vl} \in R^{V \times T \times J \times 2} \times (scale + 1) / 2 + offset, \\ scale \in R^{V \times T \times 1 \times 2}, \\ offset \in R^{V \times T \times 1 \times 2}, \end{aligned} \quad (2)$$

M_{vl} is transformed into M_{vg} , which is combined with the ground truth 2D motion M_0 to $M_g \in R^{(V+1) \times T \times (J+2) \times 2}$. The 3D motion in the world coordinate system is then optimized via triangulation [5]. Note that, following [32], to ensure multi-view consistency in the generated results, the triangulated 3D motion is reprojected into the 2D space to guide the generation at the $t + 1$ time step. At the final time step T , we obtain the 3D motion containing global positional information. Following prior methods [11, 23], we employ SMPLify [2] to fit the SMPL [20] pose parameters.

4. Experiment

4.1. Implementation

Our diffusion model is constructed with 8 transformer decoder layers, each layer having 4 heads and 512 hidden units. In pre-training, HumanML3D [4] is projected onto random viewpoints to speed up multi-view model convergence, and in-distribution 2D human data like RICH [7] can be added. This phase uses a learning rate of 1e-4, a batch size of 64, and runs for 2000 epochs. Subsequently, we fine-tune the Multi-view Diffusion model using HumanML3D [4], BEDLAM [1], and Human3.6M [8], where HumanML3D [4] includes HumanAct12 [3] and AMASS [21]. The multi-view training is configured with 4 views ($V = 4$), a reduced learning rate of 1e-5, a batch size of 39, and extends over 3000 epochs. Throughout both stages, we employ the Adam optimizer for parameter updates. The model supports a maximum sequence length of $L = 300$.

4.2. Datasets and Metrics

Evaluation datasets. Following GV-HMR [25] and MV-Lift [16], we selected RICH [7] and AIST++ [17] to evaluate our model. These two datasets are collected in real-world scenarios, encompassing both outdoor and indoor environments. They include actions such as sitting, lying down, and handstands, which are less represented in the training set, thereby providing a more comprehensive assessment of the model’s generalization capabilities.

RICH [7] comprises multi-view outdoor and indoor video sequences at 4K resolution, providing accurate 3D global motion labels. It includes 52 test scenes, with 3-4 test viewpoints per scene, totaling 191 viewpoints. Compared to other human 3D pose datasets that are mostly collected in laboratory settings, the RICH [7] dataset is derived from real-life scenarios, encompassing a wide range of human actions and interactions with the environment, such as walking, sitting, grasping, and more.

AIST++ [17] is currently the largest and most diverse 3D human keypoint annotated database. It includes 1,408 dance clips across 10 dance genres, comprising 10,108,015 frames of human images captured from 9 different camera angles. Building upon the original multi-view videos, the dataset has been annotated with 3D skeletal data.

Metrics. We follow the evaluation protocol [25, 26] to assess our model. In the camera coordinate system, we adhere to the widely used metrics: mean per-joint position error (MPJPE) and mean per-joint position error with Procrustes Alignment (PA-MPJPE). Additionally, since our model can predict absolute positions in the world coordinate system, we also compute the mean per-joint position error without root alignment, defined as Abs-MPJPE. Furthermore, we calculate W-MPJPE, which aligns the first two frames in the world coordinate system, and WA-MPJPE, which aligns the entire sequence, as well as the root translation error (T_{root}).

4.3. Lifting SMPL keypoint with ground truth

Our method supports lifting keypoints in various formats, and we begin by analyzing the widely-used SMPL [20] format in academia. Existing 3D motion prediction methods typically involve two stages: 1) detecting 2D keypoints [28, 37], and 2) predicting 3D poses from 2D keypoints [36, 39]. We focus on the second stage, estimating 3D poses given 2D keypoints, and use ground truth 2D keypoints for intuitive performance comparison. We compare our method with several baselines: 1) methods trained only on 3D data, such as WHAM [26] and GV-HMR [25], which predict 3D motion directly from videos and 2D keypoints; 2) state-of-the-art 2D-to-3D lifting models like MotionBERT [39]; 3) optimization-based methods like SMPLify [2], which optimize using 2D reprojection loss; and 4) methods using external environmental information to predict absolute world

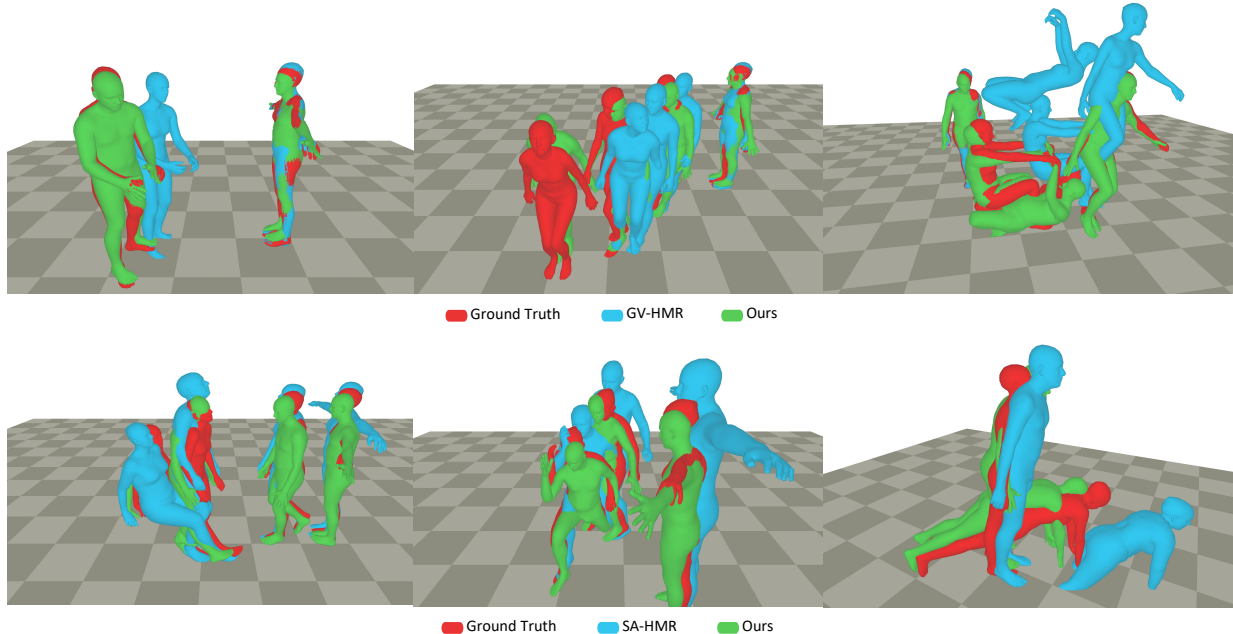


Figure 4. **Qualitative comparison on RICH [7].** The first row represents the global motion after alignment in the camera coordinate system for the first frame, and the second row represents the absolute positions in the world coordinate system.

Methods	PA-MPJPE	MPJPE	Abs-MPJPE	W-MPJPE	WA-MPJPE
SMPLify [2]	95.4	185.4	525.3	353.3	252.2
MotionBERT [39]	123.1	146.1	—	—	—
SA-HMR [24]	51.1	93.2	268.3	—	—
WHAM [26]	40.2	74.3	—	182.3	106.0
GV-HMR [25]	33.6	58.9	—	110.0	68.4
GV-HMR [25]+SMPLify [2]	27.4	50.6	395.8	88.0	56.9
Ours	25.8	38.7	152.5	85.3	56.1

Table 1. **Quantitative results on RICH [7].** PA-MPJPE and MPJPE compute errors in the camera coordinate system, while Abs-MPJPE, W-MPJPE, and WA-MPJPE compute errors in the world coordinate system.

coordinates, such as SA-HMR [24]. For fairness, we replace all baselines’ 2D keypoint inputs with ground truth.

We chose the RICH [7] dataset for motion testing due to its diverse actions, like push-ups and inclined pull-ups, which are outside conventional training distributions, enabling better evaluation of 3D motion methods’ generalization. To simulate the practical application process of our proposed framework, we included the RICH [7] training set during the 2D pretrain phase, where only a randomly selected single view of 2D motion was used for training in each batch. However, it is important to note that we do so to demonstrate our ability to effectively utilize the 2D phase to enhance model performance, and it is not necessary to include the homologous training set to surpass the baselines. Results without the inclusion of any additional data are further discussed in Sec. 4.5.

The quantitative results are presented in Tab. 1, demon-

strating that our method achieves the best performance across all metrics. For the MotionBERT [39], which also employs a 2D lift to 3D approach, its generalization capability appears to be inferior, possibly due to the lack of training on homologous data. Compared to WHAM [26] and GV-HMR [25], our method reduces the PA-MPJPE by 14.4mm and 7.2mm, respectively. In comparison with GV-HMR [25], our method also outperforms it in terms of global trajectory, especially considering that GV-HMR [25] cannot output absolute positions. GV-HMR [25] + SMPLify [2] serves as a significant baseline. We utilize the results from GV-HMR [25] as the initialization for SMPLify [2], optimizing with 2D ground truth as the loss function and providing real camera parameters. This state-of-the-art method combined with optimization yields the best results among existing methods and maintains consistency with our inputs. As shown in the table, our results still hold an advantage. SA-HMR [24] has the most similar inputs to ours, allowing for a direct comparison of Abs-MPJPE, which does not align with the ground truth. It is evident that our error in absolute position is significantly smaller than that of SA-HMR [24]. Moreover, our spatial constraints do not require any additional equipment for data collection; only camera annotation is needed, which greatly reduces application costs and enables lightweight deployment in any scenario.

A qualitative comparison is illustrated in Fig. 4. The first row demonstrates the comparison with GV-HMR [25] after aligning the first frame. Since our method can encode

Methods	PA-MPJPE	MPJPE	T_{root}
ElePose [34]	251.1	269.4	—
MAS [11]	155.6	191.1	—
SMPLify [2]	146.7	171.6	77.4
MotionBERT [39]	108.6	134.0	101.6
WHAM [26]	75.1	104.8	164.3
GV-HMR [25]	69.3	120.9	291.6
MVLift [16]	79.2	110.7	67.6
Ours	60.5	92.4	64.7

Table 2. **Quantitative results on AIST++ [17].**

spatial positional relationships, our trajectory is more accurate than GV-HMR [25] in each subsequent frame. The second row shows the difference in absolute positions between our method, SA-HMR [24], and the ground truth. With the same external environment input, our motion aligns more closely with the ground truth, and both the position and scale are more reasonable. The results demonstrate, we only need to annotate 2D data to generate metric-accurate 3D poses as ground truth for the training of downstream tasks.

4.4. Lifting COCO keypoint with detector

To demonstrate the effectiveness of different keypoint formats, we also trained a COCO version of the lift model and present the results in this section using the 2D detector ViTPose [37] as input. We selected AIST++ [17] as the testset, which provides 3D ground truth in COCO format. Following [16], we compared our approach with several baselines, including MotionBERT [39], WHAM [26], GV-HMR [25], ElePose [34], SMPLify [2], MAS [11], and MVLift [16]. Among these, ElePose is also a 3D pose lifting method. The input for the baselines is also ViTPose [37]. Unlike MVLift [16], to better illustrate the generalization capability of our method, we did not use any AIST++ [17] training data during the 2D pretrain and multi-view fine-tuning in this version.

The quantitative results are presented in Tab. 2. MVLift [16] incorporated AIST++ [17] as a training set during the 2D phase, which enhances the diffusion model’s ability to learn the generation of homologous dance movements. Even without exposure to similar data, our model significantly outperforms MVLift [16] in terms of PA-MPJPE results, and our global trajectory is also optimal. Although we trained with similar data as WHAM [26] and GV-HMR [25], our generalization results are still superior. Additionally, we can still incorporate 2D data with scene-specific distribution on this basis, which facilitates extending our model to real-world application scenarios.

4.5. Ablation study

We conducted ablation experiments on the RICH [7] for Mpcap-2-to-3, and the comparative results are presented in Tab. 3. Lines 1-3 in Tab. 3 illustrate the differences when adding ground pointmaps as constraints. Previously, in-

Methods	PA-MPJPE	MPJPE	Abs-MPJPE	W-MPJPE	WA-MPJPE
No-pointmaps	45.8	85.6	373.9	121.8	77.0
Ours	30.5	45.3	155.9	88.6	57.9
Ours+RICH(2D)	25.8	38.7	152.5	85.3	56.1

Table 3. **Ablation studies on RICH [7].**

accuracies in the global position from a single viewpoint could affect the overall pose during multi-view triangulation, pulling the motion off course and further impacting PA-MPJPE. After incorporating the ground equation, the global absolute position error significantly decreased, and the convergence speed was greatly accelerated. Additionally, we compared the results of adding and not adding homologous data training during the 2D phase (lines 2-3). It can be observed that adding homologous data led to significant improvements in PA-MPJPE and MPJPE, demonstrating that in our method, collecting only 2D data can enhance the performance of 3D motion. Moreover, even without training on homologous data, the model’s metrics still outperform those of the baselines listed in Tab. 1, proving that our method has a fundamental and absolute advantage.

4.6. Limitation and future work

Although our method shows competitive results, some limitations remain. While we enhance 3D motion from 2D videos, the accuracy of 2D SMPL skeleton prediction from videos is insufficient, impacting 3D motion estimation. In practical applications, we currently rely on manually annotated 2D poses, which incurs labor costs, or we use more accurate COCO format poses generated by ViTPose [37] to lift to 3D poses. In the future, we aim to optimize the 2D motion prediction model for better results. Additionally, our application is limited to fixed camera scenarios, and exploring global 3D motion prediction in moving camera setups will be part of our future research.

5. Conclusion

In this paper, we introduce Mocal-2-to-3, a novel framework for predicting global 3D motion sequences from monocular inputs. The key contribution is that we enhance prediction results on the corresponding test set by pre-training solely with 2D data from the same source as the test scene, while ensuring scientifically consistent human body structures through multi-view fine-tuning. We also propose an improved motion representation, incorporating decomposed actions, positional information, and pointmaps to recover more reasonable global locations. Our approach effectively utilizes accessible 2D data and mitigates depth ambiguity in monocular global position prediction. Experimental results demonstrate the potential of our method to improve 3D motion estimation in out-of-distribution scenarios using only supplementary 2D data, offering a promising direction for future research in this domain.

References

- [1] Michael J Black, Priyanka Patel, Joachim Tesch, and Jinlong Yang. Bedlam: A synthetic dataset of bodies exhibiting detailed lifelike animated motion. In *Proceedings of the IEEE/CVF Conference on Computer Vision and Pattern Recognition*, pages 8726–8737, 2023. 2, 6
- [2] Federica Bogo, Angjoo Kanazawa, Christoph Lassner, Peter Gehler, Javier Romero, and Michael J Black. Keep it smpl: Automatic estimation of 3d human pose and shape from a single image. In *Computer Vision—ECCV 2016: 14th European Conference, Amsterdam, The Netherlands, October 11–14, 2016, Proceedings, Part V 14*, pages 561–578. Springer, 2016. 6, 7, 8
- [3] Chuan Guo, Xinxin Zuo, Sen Wang, Shihao Zou, Qingyao Sun, Annan Deng, Minglun Gong, and Li Cheng. Action2motion: Conditioned generation of 3d human motions. In *Proceedings of the 28th ACM International Conference on Multimedia*, pages 2021–2029, 2020. 6
- [4] Chuan Guo, Shihao Zou, Xinxin Zuo, Sen Wang, Wei Ji, Xingyu Li, and Li Cheng. Generating diverse and natural 3d human motions from text. In *Proceedings of the IEEE/CVF Conference on Computer Vision and Pattern Recognition*, pages 5152–5161, 2022. 5, 6
- [5] Richard I Hartley and Peter Sturm. Triangulation. *Computer vision and image understanding*, 68(2):146–157, 1997. 6
- [6] Jonathan Ho, Ajay Jain, and Pieter Abbeel. Denoising diffusion probabilistic models. *Advances in neural information processing systems*, 33:6840–6851, 2020. 5
- [7] Chun-Hao P Huang, Hongwei Yi, Markus Höschle, Matvey Safroshkin, Tsvetelina Alexiadis, Senya Polikovsky, Daniel Scharstein, and Michael J Black. Capturing and inferring dense full-body human-scene contact. In *Proceedings of the IEEE/CVF Conference on Computer Vision and Pattern Recognition*, pages 13274–13285, 2022. 2, 6, 7, 8
- [8] Catalin Ionescu, Dragos Papava, Vlad Olaru, and Cristian Sminchisescu. Human3.6m: Large scale datasets and predictive methods for 3d human sensing in natural environments. *IEEE transactions on pattern analysis and machine intelligence*, 36(7):1325–1339, 2013. 2, 6
- [9] Jia Jinrang, Zhenjia Li, and Yifeng Shi. Monouni: A unified vehicle and infrastructure-side monocular 3d object detection network with sufficient depth clues. *Advances in Neural Information Processing Systems*, 36:11703–11715, 2023. 5
- [10] Angjoo Kanazawa, Michael J Black, David W Jacobs, and Jitendra Malik. End-to-end recovery of human shape and pose. In *Proceedings of the IEEE conference on computer vision and pattern recognition*, pages 7122–7131, 2018. 3
- [11] Roy Kapon, Guy Tevet, Daniel Cohen-Or, and Amit H Bermano. Mas: Multi-view ancestral sampling for 3d motion generation using 2d diffusion. In *Proceedings of the IEEE/CVF Conference on Computer Vision and Pattern Recognition*, pages 1965–1974, 2024. 3, 6, 8
- [12] Muhammed Kocabas, Nikos Athanasiou, and Michael J Black. Vibe: Video inference for human body pose and shape estimation. In *Proceedings of the IEEE/CVF conference on computer vision and pattern recognition*, pages 5253–5263, 2020. 3
- [13] Muhammed Kocabas, Chun-Hao P Huang, Otmar Hilliges, and Michael J Black. Pare: Part attention regressor for 3d human body estimation. In *Proceedings of the IEEE/CVF international conference on computer vision*, pages 11127–11137, 2021. 3
- [14] Nikos Kolotouros, Georgios Pavlakos, Michael J Black, and Kostas Daniilidis. Learning to reconstruct 3d human pose and shape via model-fitting in the loop. In *Proceedings of the IEEE/CVF international conference on computer vision*, pages 2252–2261, 2019. 3
- [15] Vincent Leroy, Yohann Cabon, and Jérôme Revaud. Grounding image matching in 3d with mast3r. In *European Conference on Computer Vision*, pages 71–91. Springer, 2024. 5
- [16] Jiaman Li, C Karen Liu, and Jiajun Wu. Lifting motion to the 3d world via 2d diffusion. *arXiv preprint arXiv:2411.18808*, 2024. 2, 3, 6, 8
- [17] Ruilong Li, Shan Yang, David A Ross, and Angjoo Kanazawa. Ai choreographer: Music conditioned 3d dance generation with aist++. In *Proceedings of the IEEE/CVF International Conference on Computer Vision*, pages 13401–13412, 2021. 6, 8
- [18] Zhihao Li, Jianzhuang Liu, Zhenyong Zhang, Songcen Xu, and Youliang Yan. Cliff: Carrying location information in full frames into human pose and shape estimation. In *European Conference on Computer Vision*, pages 590–606. Springer, 2022. 3
- [19] Tsung-Yi Lin, Michael Maire, Serge Belongie, James Hays, Pietro Perona, Deva Ramanan, Piotr Dollár, and C Lawrence Zitnick. Microsoft coco: Common objects in context. In *Computer Vision—ECCV 2014: 13th European Conference, Zurich, Switzerland, September 6–12, 2014, Proceedings, Part V 13*, pages 740–755. Springer, 2014. 2
- [20] Matthew Loper, Naureen Mahmood, Javier Romero, Gerard Pons-Moll, and Michael J. Black. SMPL: A skinned multi-person linear model. *ACM Trans. Graph.*, 2015. 3, 6
- [21] Naureen Mahmood, Nima Ghorbani, Nikolaus F Troje, Gerard Pons-Moll, and Michael J Black. Amass: Archive of motion capture as surface shapes. In *Proceedings of the IEEE/CVF international conference on computer vision*, pages 5442–5451, 2019. 2, 6
- [22] Priyanka Patel, Chun-Hao P Huang, Joachim Tesch, David T Hoffmann, Shashank Tripathi, and Michael J Black. Agora: Avatars in geography optimized for regression analysis. In *Proceedings of the IEEE/CVF Conference on Computer Vision and Pattern Recognition*, pages 13468–13478, 2021. 2
- [23] Huaijin Pi, Ruoxi Guo, Zehong Shen, Qing Shuai, Zechen Hu, Zhumei Wang, Yajiao Dong, Ruizhen Hu, Taku Komura, Sida Peng, et al. Motion-2-to-3: Leveraging 2d motion data to boost 3d motion generation. *arXiv preprint arXiv:2412.13111*, 2024. 2, 3, 5, 6
- [24] Zehong Shen, Zhi Cen, Sida Peng, Qing Shuai, Hujun Bao, and Xiaowei Zhou. Learning human mesh recovery in 3d scenes. In *Proceedings of the IEEE/CVF Conference on Computer Vision and Pattern Recognition*, pages 17038–17047, 2023. 3, 7, 8
- [25] Zehong Shen, Huaijin Pi, Yan Xia, Zhi Cen, Sida Peng, Zechen Hu, Hujun Bao, Ruizhen Hu, and Xiaowei Zhou.

- World-grounded human motion recovery via gravity-view coordinates. In *SIGGRAPH Asia 2024 Conference Papers*, pages 1–11, 2024. [2](#), [3](#), [6](#), [7](#), [8](#)
- [26] Soyong Shin, Juyong Kim, Eni Halilaj, and Michael J Black. Wham: Reconstructing world-grounded humans with accurate 3d motion. In *Proceedings of the IEEE/CVF Conference on Computer Vision and Pattern Recognition*, pages 2070–2080, 2024. [2](#), [6](#), [7](#), [8](#)
- [27] Qing Shuai, Zhiyuan Yu, Zhize Zhou, Lixin Fan, Haijun Yang, Can Yang, and Xiaowei Zhou. Reconstructing close human interactions from multiple views. *ACM Transactions on Graphics (TOG)*, 42(6):1–14, 2023. [2](#)
- [28] Ke Sun, Bin Xiao, Dong Liu, and Jingdong Wang. Deep high-resolution representation learning for human pose estimation. In *Proceedings of the IEEE/CVF conference on computer vision and pattern recognition*, pages 5693–5703, 2019. [6](#)
- [29] Qingping Sun, Yanjun Wang, Ailing Zeng, Wanqi Yin, Chen Wei, Wenjia Wang, Haiyi Mei, Chi-Sing Leung, Ziwei Liu, Lei Yang, et al. Aios: All-in-one-stage expressive human pose and shape estimation. In *Proceedings of the IEEE/CVF Conference on Computer Vision and Pattern Recognition*, pages 1834–1843, 2024. [2](#)
- [30] Yu Sun, Qian Bao, Wu Liu, Yili Fu, Michael J Black, and Tao Mei. Monocular, one-stage, regression of multiple 3d people. In *Proceedings of the IEEE/CVF international conference on computer vision*, pages 11179–11188, 2021. [3](#)
- [31] Yu Sun, Wu Liu, Qian Bao, Yili Fu, Tao Mei, and Michael J Black. Putting people in their place: Monocular regression of 3d people in depth. In *Proceedings of the IEEE/CVF Conference on Computer Vision and Pattern Recognition*, pages 13243–13252, 2022. [2](#)
- [32] Guy Tevet, , Sigal Raab, Brian Gordon, Daniel Shafir, Daniel Cohen-Or, and Amit H Bermano. Human motion diffusion model. In *In The Eleventh International Conference on Learning Representations*, 2023. [3](#), [5](#), [6](#)
- [33] A Vaswani. Attention is all you need. *Advances in Neural Information Processing Systems*, 2017. [5](#)
- [34] Bastian Wandt, James J Little, and Helge Rhodin. Elepose: Unsupervised 3d human pose estimation by predicting camera elevation and learning normalizing flows on 2d poses. In *Proceedings of the IEEE/CVF Conference on Computer Vision and Pattern Recognition*, pages 6635–6645, 2022. [8](#)
- [35] Shuzhe Wang, Vincent Leroy, Yohann Cabon, Boris Chidlovskii, and Jerome Revaud. Dust3r: Geometric 3d vision made easy. In *Proceedings of the IEEE/CVF Conference on Computer Vision and Pattern Recognition*, pages 20697–20709, 2024. [5](#)
- [36] Jinglin Xu, Yijie Guo, and Yuxin Peng. Finepose: Fine-grained prompt-driven 3d human pose estimation via diffusion models. In *Proceedings of the IEEE/CVF Conference on Computer Vision and Pattern Recognition*, pages 561–570, 2024. [6](#)
- [37] Yufei Xu, Jing Zhang, Qiming Zhang, and Dacheng Tao. Vitpose: Simple vision transformer baselines for human pose estimation. *Advances in Neural Information Processing Systems*, 35:38571–38584, 2022. [2](#), [6](#), [8](#)
- [38] Yu Zhan, Fenghai Li, Renliang Weng, and Wongun Choi. Ray3d: ray-based 3d human pose estimation for monocular absolute 3d localization. In *Proceedings of the IEEE/CVF Conference on Computer Vision and Pattern Recognition*, pages 13116–13125, 2022. [2](#), [3](#)
- [39] Wentao Zhu, Xiaoxuan Ma, Zhaoyang Liu, Libin Liu, Wayne Wu, and Yizhou Wang. Motionbert: A unified perspective on learning human motion representations. In *Proceedings of the IEEE/CVF International Conference on Computer Vision*, pages 15085–15099, 2023. [2](#), [3](#), [6](#), [7](#), [8](#)